




Article

Structural Analysis of the Sympathetic Restoration and Conservation of the Gopinath Temple, Kathmandu, Nepal

Andrés Arce ¹, Alejandro Jiménez Rios ^{2,*}, Igor Tomic ³ and David Biggs ⁴¹ UNESCO Office, Katmandu P.O. Box 14391, Nepal; aarce.cr@gmail.com² Department of Built Environment, Oslo Metropolitan University, NO-0130 Oslo, Norway³ School of Architecture, Civil and Environmental Engineering, École Polytechnique Fédérale de Lausanne, 1015 Lausanne, Switzerland; igor.tomic@epfl.ch⁴ Biggs Consulting Engineering, Saratoga Springs, NY 12866, USA; biggsconsulting@att.net

* Correspondence: alejand@oslomet.no

Abstract: The sympathetic restoration and conservation of built cultural heritage play a significant role in the management and preparedness for future climate scenarios by facilitating adaptive reuse, enhancing cultural resilience, preserving traditional knowledge, and boosting tourism. The importance of restoring damaged heritage sites after an earthquake drew international attention to Nepal after the 2015 Gorka Earthquake. UNESCO established an office in Kathmandu to promote the restoration of tangible and intangible heritage in the area. This included developing structural analyses of buildings with historical and cultural value that, due to their nature, cannot be intervened with the same methodology as modern buildings. In this paper, the case study of the earthquake-damaged Gopinath temple is discussed. First, an initial visual inspection phase and the following diagnosis of the structure are discussed. Then, the results from a series of static and dynamic structural analyses performed to determine the safety level of the structure, together with a sensitivity analysis, are presented. A sympathetic intervention proposal capable of increasing the temple's safety level, and based on the addition of timber plates, has resulted in substantial improvements in the lateral behavior of the structure. The proposed intervention is deemed sustainable and able to increase the resilience of the temple in the face of future hazards.



Citation: Arce, A.; Jiménez Rios, A.; Tomic, I.; Biggs, D. Structural Analysis of the Sympathetic Restoration and Conservation of the Gopinath Temple, Kathmandu, Nepal. *Heritage* **2024**, *7*, 3194–3210. <https://doi.org/10.3390/heritage7060151>

Academic Editor: Carolyn S. Hayles

Received: 4 April 2024

Revised: 28 May 2024

Accepted: 3 June 2024

Published: 11 June 2024



Copyright: © 2024 by the authors. Licensee MDPI, Basel, Switzerland. This article is an open access article distributed under the terms and conditions of the Creative Commons Attribution (CC BY) license (<https://creativecommons.org/licenses/by/4.0/>).

Keywords: Nepal heritage conservation; Gorka earthquake; Gopinath temple; structural analysis; safety-level assessment; sympathetic intervention proposal; sustainability

1. Introduction

The conservation of built cultural heritage is increasingly gaining recognition as a vital component in the pursuit of sustainable development goals [1–3]. Since 2015, the United Nations Educational, Scientific, and Cultural Organization (UNESCO) has established the Sustainable Development Goals (SDGs) to effectively tackle climate change as one of their aims. The value of the built cultural heritage to achieve sustainable development is specifically highlighted in SDG 11 and Target 11.4, which calls for stronger efforts to protect and safeguard the world's cultural (and natural) heritage [4]. The interplay between cultural heritage, including historic buildings, monuments, and cultural landscapes, and sustainability embodies a profound overlap of social, economic, and environmental dimensions [5–9]. This interconnection offers a rich context for examining the potential contribution of cultural heritage conservation to sustainability and resilience in the face of global challenges, such as climate change, urbanization, and socio-economic disparities [10–12]. Sympathetic restoration and conservation studies have the potential to elucidate the significance of conserving built cultural heritage in the context of sustainable development, underscoring the potential of these historical assets in achieving key sustainability goals and fostering resilience within communities. Moreover, thoughtful preservation and adaptive reuse of

heritage buildings can contribute to environmental sustainability, promote social cohesion, fuel economic growth, and enhance preparedness for future climate scenarios [13–15].

Particularly, unreinforced historical masonry buildings have demonstrated their vulnerability to different environmental and human-induced hazards [16]. Of special interest, due to the degree of damage caused to built cultural heritage and their frequent repetition, is the study of earthquakes, which have occurred on many occasions, both in the distant past and in recent history [17]. Many of the affected assets by this phenomenon are structures and monuments, possessing cultural values important for society and humanity. To develop effective seismic risk-mitigation strategies, it is necessary to develop both new assessment procedures and new retrofit solutions that respect the cultural values and adhere to ICOMOS guidelines [18,19], while being sympathetic and sustainable. The analysis of such buildings is further complicated by uncertainties faced both in terms of material and modeling properties [20,21]. Another difficulty is the use of advanced numerical tools and the interpretation of the results, which require experience, knowledge, and understanding of the software. To cope with this issue, several numerical strategies have been developed, tested, and validated by different researchers [22]. Some examples are the so-called Equivalent Frame Models (EFM) [23,24], the Block-Based Models (BBM) [25,26], the Geometry-Based Models (GBM) [27–29], and the widely spread and adopted Continuum Homogeneous Model (CHM) [30–32].

Various researchers addressed the topic of retrofitting historical monuments using traditional and modern techniques while accounting for the above-mentioned difficulties and limitations. The first group of authors performed shake-table tests on both unretrofitted and retrofitted specimens. Magenes et al. [33] tested unretrofitted two-story stone-masonry buildings using both moderate and extensive strengthening. Both interventions improved the building behavior, but the research also proved that the desired effect can be achieved using innovative and non-intrusive retrofitting techniques. Guerrini et al. [34] tested both unstrengthened and strengthened unreinforced stone masonry, considerably improving the seismic behavior by a non-invasive retrofitting intervention. A similar conclusion was reached by Vintzileou et al. [35] when performing a shake-table test on a three-leaf stone-masonry building with wooden floors. Biaxial earthquake motion was applied incrementally, until the occurrence of repairable damages. Then, the specimen was strengthened by non-invasive interventions, primarily aimed at improving the connections between floors and walls and injecting the walls. Comparing the behavior of the specimen under seismic excitations before and after strengthening shows that the intervention techniques improved the seismic behavior of the structure.

A second group of authors proposed innovative strengthening techniques for retrofitting cultural heritage buildings, both using numerical and experimental quasi-static methods. Mininno et al. [36] modeled both the in-plane and out-of-plane performances of textile-reinforced-mortar (TRM)-strengthened masonry walls. The study showed that the strengthening by using TRM layers largely improved the performance of the masonry walls, both in terms of strength and displacement capacity. Arce et al. [37] studied the improvement of shear capacity on replicas of historical masonry walls through diagonal tension tests. The authors found an increase of up to 330% in peak shear strength by reinforcing specimens with two layers of carbon textile on both faces. Other examples of advanced analysis performed on masonry structures include the study of Sabani et al. [38], which accounted for the influence of soil–structure interaction of a masonry tower located in Norway, and the work of Wang and Milani [39] on traditional pagodas by implementing a 3D distinct element limit analysis approach, which helped to determine the seismic vulnerability of this structure typology.

The case study presented in this paper is located in Kathmandu, the capital of Nepal, located in the Himalayan belt. The area is an active seismic zone, whose activity is caused by the convergent movement of the Indian plate into the Eurasian plate [40]. The interaction between these tectonic plates has caused major earthquakes that have considerably affected the country throughout its history [41]. The most recent event of considerable magnitude,

7.8 Mw, was the 2015 Gorkha Earthquake [42], which was the worst since 1934 [43]. It damaged over 800,000 buildings [44], including those that are a part of the UNESCO World Heritage Site of the Kathmandu Valley. The selected building presented in this paper corresponds to the Gopinath temple situated in Hanuman Dhoka, Kathmandu [45]. The objective was to understand the present state of damage in the temple by inspection and numerical analysis, followed by the design and numerical analysis of a retrofitting intervention that respected the temple's cultural values and practical limitations and followed a sustainable approach.

The rest of this paper is organized as follows. In Section 2, the followed methodology for performing the study of the temple's history, conducting the visual inspection, and describing the developed numerical modeling, as well as the climate-change considerations adopted, is presented. In Section 3, the results of the visual inspection, diagnosis, and structural analyses are highlighted. In addition, the retrofit intervention was selected, and the safety-level assessment of the temple that was achieved is also discussed in this section. The retrofitting intervention proposed and the effects on the structure are demonstrated using advanced numerical tools. Finally, in Section 4, conclusions based on the conducted work are reported.

2. Methodology

2.1. Historic Research

Historical research in the context of built cultural heritage conservation refers to the systematic investigation into the history and significance of a heritage building or site. This includes studying its origins, the purpose for its construction, the architectural styles and techniques used, changes made over time, and the socio-cultural context of its era [46]. This is the first activity recommended by the ISCARSAH guidelines on the analysis, conservation, and structural restoration of architectural heritage [47]. Information about the temple's origin, phases of construction, and modifications was obtained from the local library of the UNESCO office in Kathmandu. The collection included books about traditional architecture and a report about previous interventions at this temple [48].

2.2. Visual Inspection

Visual inspection refers to the systematic observation and examination of a heritage building or site to assess its current condition, understand its construction and materials, and identify any signs of damage or deterioration [49]. The inspection campaign for the temple took approximately two days, starting from the exterior at the plinth level and documenting all the structural elements up to the highest level. The information was collected on paper, and photographs were later used to put together a damage-assessment set of plans that describe in detail all the pathologies and structural deficiencies affecting the temple by the time of the visit (July 2017).

2.3. Numerical Modeling

The type of numerical analysis chosen for this study was the finite-element method (FEM), following a macro-model approach [22]. The numerical analysis was performed using ANSYS version 17.1. Solid65 (iso-parametric tridimensional 8 node) elements were chosen to model the masonry walls, as this type of finite element allows for the simulation of crushing and cracking behavior. Beam elements were chosen to represent the timber elements of the temple. Finally, roof mud and tile weight were idealized as death weight, and the corresponding load was applied directly to the masonry walls.

The structural analysis consisted of three main phases. In the first phase, the current state of the structure with no intervention was analyzed. This phase was meant to indicate whether the building needed any intervention or if failure was caused, not because of a lack of capacity but because of the deterioration of materials or another external agent. Once the source of damage had been determined, the second phase was conducted. It dealt with the design of a sympathetic retrofit proposal that would increase the safety of the building

against seismic actions while respecting sustainable principles. The final phase involved the structural analysis of the building, including the retrofit proposal. The new numerical model results were validated, and it was verified that the subjacent structural problems of the temple were resolved by this intervention.

2.4. Climate-Change Considerations

When considering the conservation of built cultural heritage, several environmental aspects are crucial. Of particular importance for the study case presented in this paper was the use of sustainable materials and practices, as the use of sustainable, locally sourced materials and energy-efficient practices in the conservation process can reduce the environmental impact of the designed retrofit intervention [50]. The proposed retrofitting techniques are based on the premise of resourcing materials and expertise locally. Avoiding the transportation of foreign components not only resulted in a high level of acceptance of the retrofit proposal but also in a CO₂ savings related to the transport of foreign materials, tools, and workers.

3. Results and Discussion

3.1. Temple History and Characteristics

The Gopinath temple was donated as a state temple by a royal patron. Based on a study of the details and stylistics of the carved elements, it is believed that the temple was built in the Malla period, between 1641 AD and 1674 AD.

Gopinath is a tiered roof temple (approximately 11 m tall) standing upon a raised square brick plinth (approximately 3 m high). The ground floor is composed of an inner unreinforced masonry wall constructed with fired clay bricks, with four door openings and a walkway between it and an outer timber colonnade. The masonry wall provides the main load-bearing system, whereas timber elements form the main roof structure [51]. The temple's structure is shown in Figure 1. The brick masonry was constructed with mud mortar. Following the 1934 destruction, the lowest level was reconstructed with lime mortar for the ground level, and mud mortar was used for the upper levels.

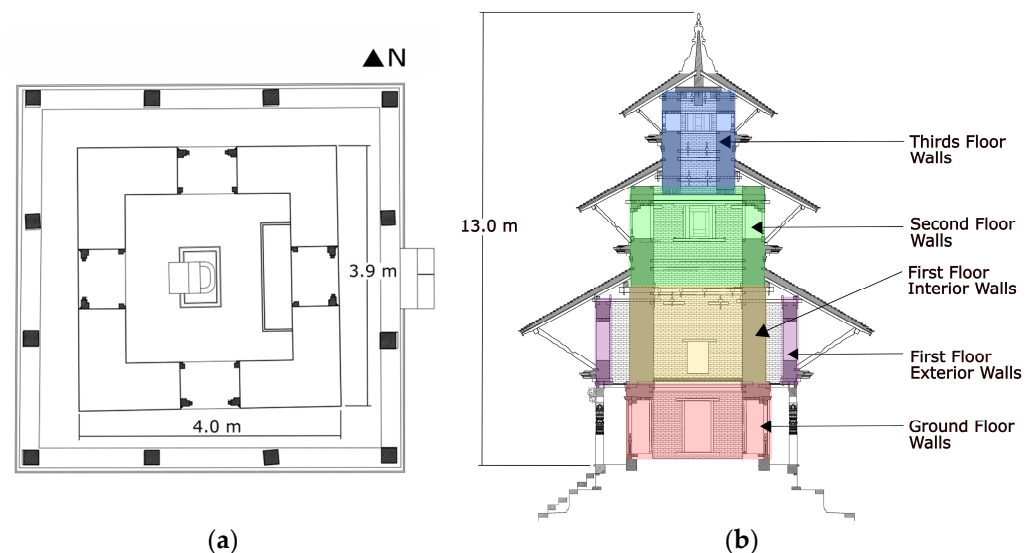


Figure 1. Gopinath temple. (a) Plan view layout of ground floor; (b) Cross-section view. Drawings created based on plans drawn by architect Purushottam Awal.

There is no documentation of the condition or repairs prior to the 1934 Nepal–Bihar earthquake, which brought the structure to the ground. Our knowledge of the temple begins after the entire structure collapsed to the plinth level during the Nepal–Bihar 1934 earthquake and was reconstructed two years later [52].

The lack of resources and urgency to proceed with repair works resulted in a rushed intervention in 1936, characterized by a not-so-strict adherence to the temple's previous historical configuration. The following restoration in 2004 attempted to correct the deviances in the historical repairs performed in 1936. The philosophy of this new intervention was based on keeping as much of the original historic fabric as possible as well as concealing any strengthening performed with modern materials. The strengthening strategy focused greatly on repairing and strengthening the structure's joints, as these elements were identified as the weakest in the structural system. Despite efforts to fix the structural deficiencies in the 2004 intervention [53], the Gopinath temple suffered several damages during the Gorkha earthquake in 2015 [54].

3.2. Visual Inspection Report

The most severe damage can be seen at the ground-level masonry walls, which have diagonal cracks, 1 to 30 mm wide, and crushing at the lower corners. Figure 2a shows a crack at the ground level in the interior wall, Figure 2b shows the same crack extended up to the exterior face. Furthermore, the exterior masonry leaf at the ground-level wall separated and moved out-of-plane up to 90 mm.



Figure 2. Shear cracks at ground level: (a) interior perspective; (b) exterior perspective.

It is likely that the detachment of the outer masonry layer is a result of incompatibility between the structural inner layer built with regular bricks, known in the local language as Ma-Apa, and the outer façade layer named Dachi-Apa (Figure 3). The inner-layer brick type can be considered as an equivalent of Western-style burnt clay bricks, while the outer bricks (Dachi-Apa) type is an iconic type of structural component characterized by a trapezoidal cross section, created with the intention of obtaining the minimum size of the outer joint. The use of these bricks in the outer façade can produce an almost nonexistent joint, which is beneficial in terms of reducing the exposure of the mortar to rain and other eroding agents. The detachment occurred despite the addition of new interlocking bricks during the 2004 intervention.

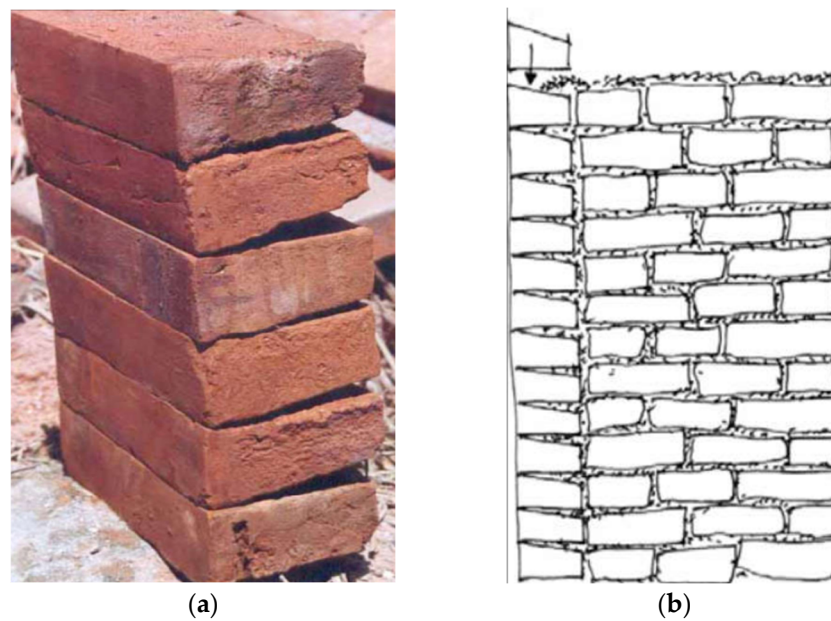


Figure 3. Dachy-Apa bricks: (a) photo of bricks stacked over each other; (b) cross section of ground-level masonry wall showing the Dachy-Apa bricks covering the façade.

The exterior wall at the first level shows severe out-of-plane movement at the upper middle section; the variation of mortar between the lower and upper parts (Figure 4a) suggests that previous repairs were performed in this section. It is likely the upper wall was rebuilt after the 2004 intervention due to similar out-of-plane damage as that observed at the present moment. The present damage is evident by the relative displacement between the exterior masonry wall and the crown timber beam. The beam was clearly meant to prevent this movement, but the existing damage proves its inefficiency in fulfilling this role. The lack of strength in the masonry resulted in the sliding of the upper bricks' layers, allowing movement of the biggest portion of the upper wall, while the top layer of bricks was held in place by the timber plate.



Figure 4. Exterior wall damages: (a) evidence of previous repairs; (b) relative out-of-plane displacement between upper timber crown beam and masonry wall.

Timber connections were highly affected and showed a permanent deformation with big openings at the joints. Timber columns show torsional movement and tilting as well. The temple has been propped and shored since 2015, as shown in Figure 5.



Figure 5. Gopinath temple's current state (2017).

3.3. Finite-Element Model and Structural Analysis

A 3D finite-element model (see Figure 6) was created to study the structural response of the temple under seismic loads and to evaluate the efficiency of the retrofit intervention proposed. All simulations were performed using ANSYS®. The geometry of the model was directly created using the native tools provided in Ansys Workbench and was based on the detailed information available from architectural plans (see Figure 1).

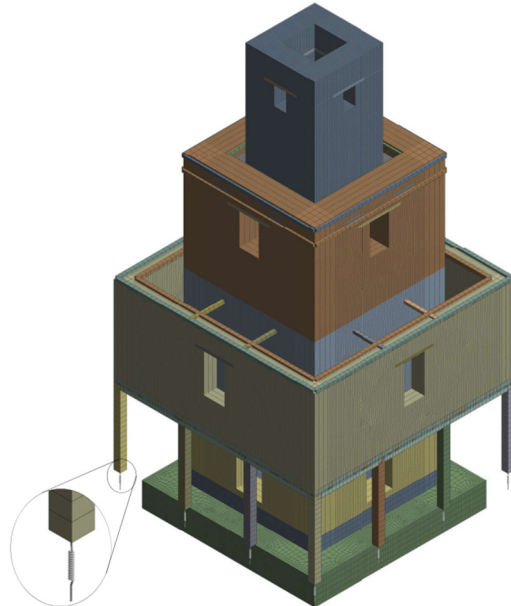


Figure 6. A 3D view of the finite-element model of the Gopinath temple, including a zoom in of the timber column base spring connection.

The assumptions adopted to model the masonry material of the temple followed a macro-model approach. Isoparametric Solid65 eight-node hexahedral elements, with three degrees of freedom at each node, were used to model the walls. The material model for masonry is based on the Willam Warnke theory [55] available in ANSYS®, which allows the masonry to crack and crush. Cracking behavior is handled through two parameters. The shear transfer coefficient for open cracks represents a shear strength reduction factor

for those subsequent loads that induce sliding across the crack face while the crack is still open. Similarly, the shear transfer coefficient for closed cracks penalizes the shear transfer at the crack location, when the crack has been closed. The values chosen are within the allowed range (zero and one) and respect the relation of the closed crack coefficient being greater than the open crack coefficient. On the other hand, crushing is idealized as the complete deterioration of the structural integrity of the material. Thus, the contribution to the stiffness of an element at the integration point in question is ignored.

This failure criterion is expressed as a function of the masonry compressive stress, f_c . F is a function of the principal stresses, and S represents the spatial failure surface (see Equation (1)). For a further description of the implementation of the William Warnke theory within the ANSYS 18.1[®] software, the software documentation can be consulted [56].

$$F/f_c - S \geq 0, \quad (1)$$

Although this is a nonlinear constitutive model, its behavior description is not based on a stress–strain curve but rather on a series of parameters that describe the material–failure criteria under a multiaxial stress state [57]. This material has been satisfactorily used to model the nonlinear response of masonry [58–60]. On the other hand, linear elastic beam finite elements were used to model the timber structural elements of the temple.

The non-structural elements of the roofs were indirectly included in the model as distributed mass applied to the top of the corresponding story walls, but the limited stiffness that such elements may contribute to the structural response was neglected. The self-weight of all structural elements represented in the model was also considered in the analysis.

The ground floor wall base was modeled as simply supported. The boundary condition for the timber column was modeled as no lateral displacement combined with a spring that prevents penetration to the ground but allows uplift. The decision to use springs is based on the type of connections used in Nepali architecture, where timber columns have a small wood pin carved at the base and are set in a stone base. This type of connection prevents lateral displacement but no uplift. The values adopted for the material mechanical properties are presented in Table 1.

Table 1. Mechanical properties used in the FEM model.

Property	Masonry	Timber
Density (kg/m ³)	1800.00	800.0
Young's modulus (MPa)	250.00	12,500.0
Poisson's ratio (–)	0.24	0.3
Uniaxial compressive strength (MPa)	1.00	-
Uniaxial tensile Strength (MPa)	0.05	-
Shear transfer coefficient for open cracks	0.30	-
Shear transfer coefficient for closed cracks	0.80	-

Finally, different meshing controls were applied to the model based on the element type (i.e., solid, or linear). The high geometrical complexity of the model with all the linear elements and their correspondent connections, along with the relatively small finite-element size selected for wall meshing (5 cm), resulted in a relatively large model with over 400 thousand nodes. The average finite-element quality value obtained was 0.609. This metric can vary between zero and one, with one being a perfect cube or square element, while zero represents a zero- or negative-element volume value.

3.3.1. Modal Analysis and Calibration of the Model

For this study, the numerical model was calibrated using as a reference the natural frequencies measured in situ by Japanese researchers from the Tokyo National Research Institute for Cultural Properties [48], hereby known as TNRICP, and the experimental values measured in a similar temple (Radha Krishna temple in Patan, Kathmandu). The calibration process adopted followed a trial-and-error approach informed by engineering judgment and considering the experimentally found natural frequencies and did not require the use of modal assurance criteria, as normally conducted in practice by conservation professionals [61].

As recommended by Jaishi et al. in 2003 [54] and further supported by Shakya [62], the modulus of elasticity of mud masonry was initially estimated at 800 MPa, with a Poisson's ratio of 0.12. The experimental frequencies reported for the first, second, and third natural frequencies of the building correspond to 2.0 Hz, 4.5 Hz, and 7.4 Hz (see Table 2 and Figure 7). The computer model's estimated frequencies are reported in the same table. However, upon comparison with the experimental results from the 2015 micro-tremor measurements conducted on site (considered as the benchmark values), it became evident that the disparity between the experimental and computer-model values exceeded 100%. This discrepancy prompted a refinement of the model to better reflect the actual behavior of the Gopinath Temple. Consequently, adjustments were made to the modulus of elasticity values until a closer correlation between the experimental and the computer-model results was achieved. The recalibrated modal frequencies are detailed in Table 2, with the discrepancy now reduced to less than 5%.

Table 2. Modal frequencies for the Gopinath temple: experimental results and numerical model results before and after calibration.

Natural Frequency	Micro Tremor Results	Computer Model before Calibration	Difference in Percentage	Computer Model after Calibration	Difference in Percentage
Mode 1	2.00	4.63	131.50%	2.00	0.00%
Mode 2	4.50	9.51	111.33%	4.27	5.11%
Mode 3	7.40	- *	- *	7.31	1.22%

* The third natural frequency of the uncalibrated model is not reported in the table, as its mode shape was different from the one found in the calibrated model.

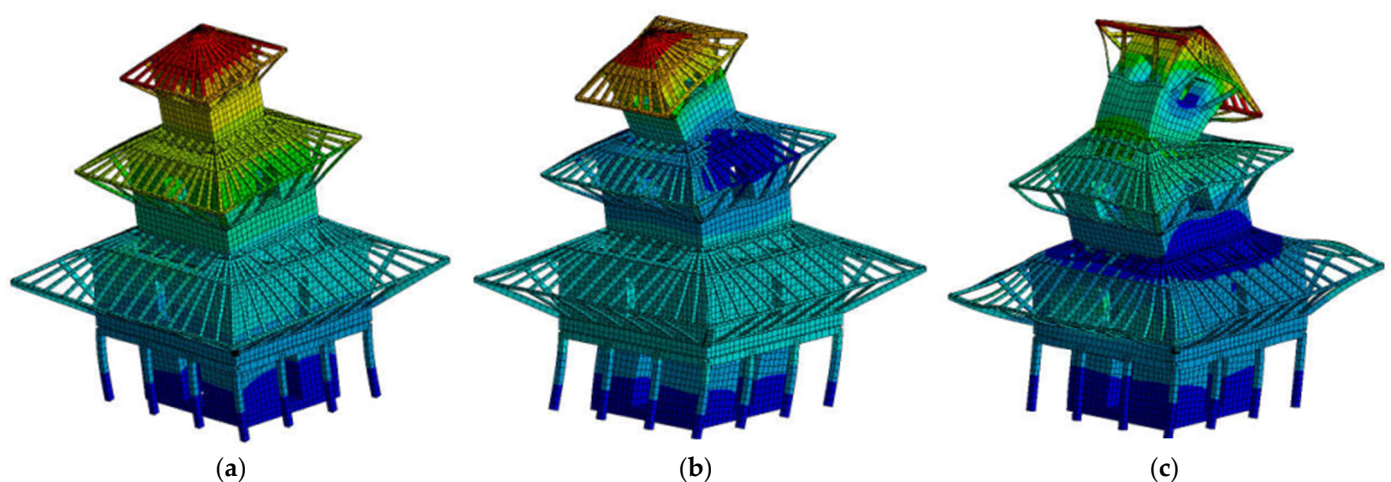


Figure 7. Modal shapes obtained from the calibrated Gopinath temple model: (a) first mode; (b) second mode; (c) third mode.

The calibration process was guided by the premise that the actual material properties of mud masonry should fall within the range of values reported by Parajuli (2012) [51] and the findings of the UNESCO testing campaign on mud masonry conducted in 2017. Parajuli suggested a modulus of elasticity for mud masonry around 274 MPa, while the UNESCO campaign indicated a range between 87–150 MPa. Gavrilovich’s research on similar mud-mortar clay-brick masonry walls reported a range of modulus of elasticity between 120 and 220 MPa [49]. Notably, the results from the destructive tests conducted by UNESCO yielded lower values compared to those reported by other researchers. Given that the lower levels of the Gopinath Temple have experienced more damage than the upper levels, it is inferred that the damaged floors exhibit a lower modulus of elasticity.

Various combinations of modulus of elasticity were iteratively tested in the computer model until the deviation between the experimental (Japanese results) and the computer-reported values fell below 5%. The finalized values of the modulus of elasticity, resulting in the minimal difference between the experimental and the computer-model results, are summarized in Table 2. Additionally, a Poisson’s ratio of 0.24 was uniformly selected for the masonry at all levels, while a value of 0.3 was chosen for timber. By comparing the modulus of elasticity values obtained after calibration for each floor to the standard value of sound masonry (250 MPa), a quantification of damage was obtained.

3.3.2. Pushover Analysis

The structural response is evaluated through its acceleration–displacement curve, which represents the value of the applied horizontal action in relation to the displacement of the control point. The top point of the structure was chosen as the control point. While showing a high degree of symmetry, there is an additional opening in the south wall on the first floor, which results in slightly less stiffness in the east–west direction. Thus, the pushover analysis was performed in the east–west direction, as this is the more critical direction and corresponds with the displacement direction of the first mode shape of the temple. Figure 8 shows that, at approximately 0.09 g, the increment of displacement starts to become non-linear, and above 0.17 g, the displacement approaches the collapse condition and is used as an indicator of the structure capacity. The Ghoroka earthquake from 2015 had a peak ground acceleration of 0.16 g and, as expected, resulted in heavy damage to the structure. Figure 9 shows the total equivalent strain as a measure of crack opening and compares it to the crack patterns found in the damage-assessment phase (damage produced by the Ghoroka earthquake). The model shows a good correlation, even though the pushover analysis cannot fully replicate the complex load scenario that generated this type of damage [63].

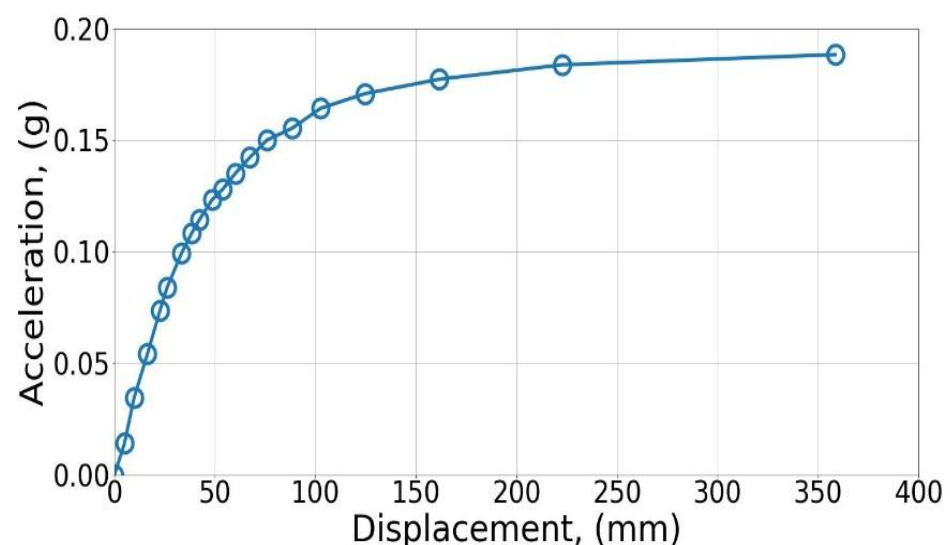


Figure 8. Pushover curve for the Gopinath temple without retrofit.

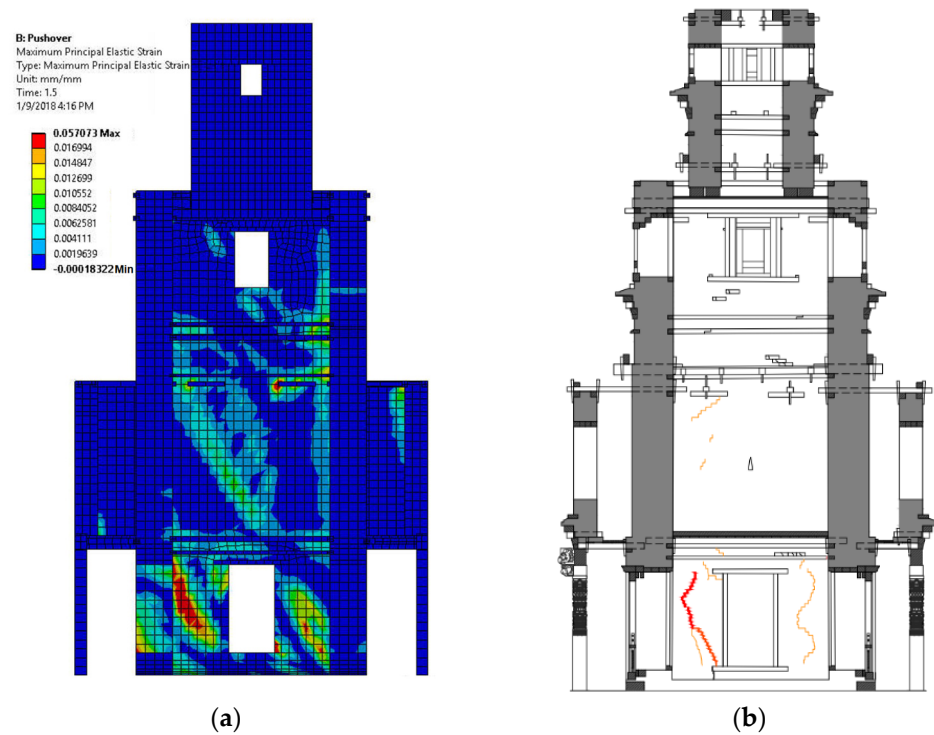


Figure 9. Comparison of (a) total strain as a measure of crack development and (b) real crack damage.

The structure features two timber beams on each face, facilitating horizontal load transfer between the interior and exterior walls at the first-floor level. However, the load transfer capacity of this connection appears inadequate due to a highly concentrated load path. This stress concentration is evident and resulted in elevated tensile and compression stresses at the beam ends (see Figure 10). Evidence of this issue manifests in the form of crushed or broken bricks and peg connectors, as illustrated in Figure 11.

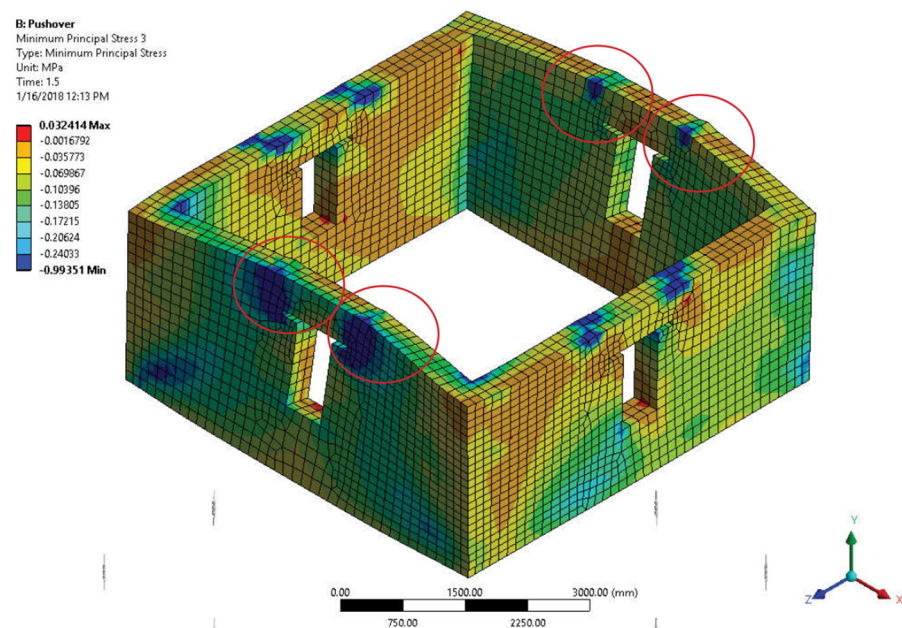


Figure 10. Concentration of stress in timber beam connectors between inner and outer wall at first-floor level.



Figure 11. Broken bricks in contact area between peg and masonry wall at first-floor level.

Clear evidence of repair work on the upper section of the exterior wall on the first floor is observed, where previous interventions utilized a mortar type differing from the original (as discussed in Section 3.2). A numerical model was constructed to simulate a scenario devoid of connectors between the interior and exterior walls, representing a situation where these connectors either failed or were absent altogether. Analysis of this model (as depicted in Figure 12) reveals the appearance of cracks at the corners, suggesting the potential for detachment at the wall's apex and consequent out-of-plane damage, akin to the findings of the damage assessment reported in the visual inspection report in Section 3.2.

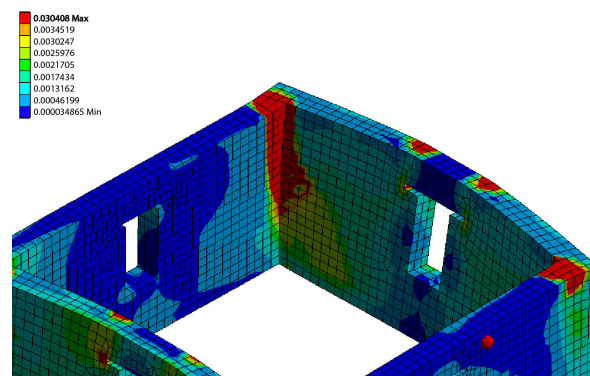


Figure 12. Total strain as an indicator of damage to the exterior wall at the first-floor level.

3.3.3. Retrofit Proposal

Due to the high seismic activity in the Kathmandu Valley, the Nepalese building code imposes high requirements for seismic design. The temple is required to prevent full collapse against earthquakes, with peak ground accelerations up to 0.30 g [64]. The traditional way of reinforcing masonry structures in Nepal is based on the addition of timber plates. These plates are timber elements embedded in masonry walls (a line of bricks is removed, and the timber plate is installed in its place) to create rings. The timber rings (also known in the literature as timber laces) provide shear capacity and improve the box behavior of the building. Therefore, the presented proposal of repair is based on this traditional construction technique, which consists of adding three wall plates at the ground level and four at the first level (see Figure 13b). The timber plates were modeled in ANSYS® as beam elements using the BEAM188 finite-element type, and their connection to the masonry walls was implemented using bonded contact, thus, matching the degree of freedom of these elements with those of the masonry walls. The retrofit proposal also

suggested an increase in masonry capacity from the current value of 1 MPa in compression to 2 MPa by reconstructing the ground- and first-floor masonry walls using a stronger lime-based mortar compatible with the existing fire clay units.

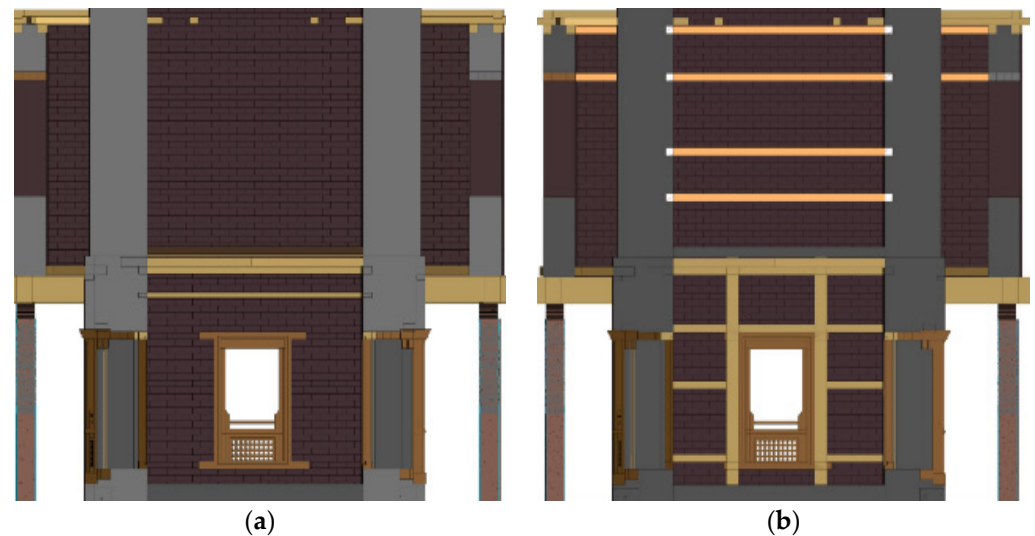


Figure 13. Retrofit proposals for the Gopinath temple: (a) original; (b) timber and steel.

Figure 14 shows the acceleration–displacement curves for the temple in its damaged (original) and retrofitted state. As can be seen in the case of the unreinforced model, failure initiates at a seismic coefficient of 0.17 g. In the case of the reinforced model, as seen in the acceleration–displacement curves in Figure 14, the reinforcement has proven to be effective, with failure initiation approximately around 0.3 g. This increase in the seismic coefficient in comparison to that for the unreinforced model is significant. The pushover analysis proves the intervention proposals to be effective, improving the building resistance to the horizontal forces, without a significant loss of ductility. By comparing the displacement that both the original and the retrofitted models would experience under a similar peak ground acceleration as the one recorded under the Ghorka earthquake, which was 0.16 g, it can be observed that the retrofitted model would be 350% stiffer than the original unreinforced temple. This observation proves the effectiveness of the strengthening strategy suggested.

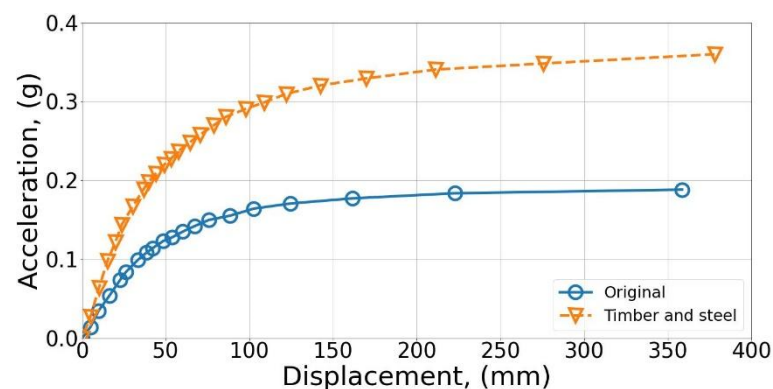


Figure 14. Acceleration–displacement curves for the Gopinath temple before and after retrofit.

Furthermore, by improving the compressive strength of the masonry walls on the ground- and first-floor levels, which is where the higher levels of load are concentrated, along with the enhanced load transfer effect of the newly incorporated timber rings along the walls' perimeter, the concentration of stresses (see Figure 10) and the consequently induced strains (as presented in Figure 12) would be reduced to acceptable values without fundamentally affecting the structural configuration of the temple. This ensures the sympla-

thetic nature of the intervention proposed, which is respectful of the local materials and construction techniques in Nepalese culture.

In contrast with Western society where maximum conservation of the original fabric is a key consideration, some Eastern cultures allow for the dismantling and reconstruction of building parts to repair or strengthen an important structure. In this proposal, the ground floor would have to be rebuilt, the bricks are to be salvaged and reused and even the recovered mud mortar can be put to use again. The reutilization of local materials, the introduction of local timber reinforcing elements, and the minimum addition of steel components result in an intervention that is agreeable to the community and drastically decreases the environmental impact associated with the transportation of foreign materials.

4. Conclusions

This paper dealt with the seismic response of Gopinath temple in Kathmandu, Nepal. First, analyses were performed on a damaged and un-retrofitted structure to understand the remaining seismic capacity of the structure. The modal analysis allowed for calibrating the material properties for the FEM analysis by the selected modulus of elasticity, which allows for a good correlation between the experimental and modeled modal frequencies and also shows a good correlation with the material test results. A retrofit proposal was modeled, and a pushover analysis was executed. The analysis showed how the addition of timber plates can substantially improve the lateral behavior of the structure while adhering to sustainable practices by using locally available materials and craftsmanship. Thus, it is concluded that the Gopinath temple structure can be provided with a high level of safety by relying on traditional Nepali construction techniques and locally sourced materials.

In conclusion, the structural analysis of the Gopinath Temple in Kathmandu, Nepal, has proven to be instrumental in guiding its sympathetic restoration and conservation. The study has illuminated the intricate details of the temple's architectural design, the materials used, and the traditional construction techniques employed, all of which hold significant cultural value. It has also shed light on the structural vulnerabilities of the temple, enabling the development of targeted restoration strategies to retrofit the structure without compromising its historical integrity.

In recent years, the field of built cultural heritage conservation has suffered a radical transformation towards digitalization of the activities conducted to ensure adequate preservation of such valuable assets. These changes are particularly fostered by international policies and strategies, such as the novel Industry 5.0 paradigm adopted by the European Union [65]. Thus, avenues for future research could be focused on determining how Industry 5.0 principles and enabling technologies could enhance conservation practice.

Author Contributions: Conceptualization, A.A., A.J.R. and I.T.; methodology, A.A., A.J.R. and I.T.; software, A.A.; validation, A.A. and D.B.; formal analysis, A.A.; investigation, A.A., A.J.R. and I.T.; writing—original draft preparation, A.A. and A.J.R. writing—review and editing, D.B.; supervision, D.B.; project administration, A.A. and A.J.R.; funding acquisition, A.J.R. All authors have read and agreed to the published version of the manuscript.

Funding: The APC was funded by Oslo Metropolitan University.

Data Availability Statement: The original contributions presented in the study are included in the article; further inquiries can be directed to the corresponding author.

Acknowledgments: To Purushottam Awal for the development of three-dimensional models that allowed for an understanding of the structure and to Alina Tamrakar for her great contribution to the damage assessment of the structure.

Conflicts of Interest: Author David Biggs was employed by the company Biggs Consulting Engineering. The remaining authors declare that the research was conducted in the absence of any commercial or financial relationships that could be construed as a potential conflict of interest.

References

1. United Nations. Tracking Progress towards Inclusive, Safe, Resilient and Sustainable Cities and Human Settlements, SDG 11 Synthesis Report. 2018. Available online: <https://uis.unesco.org/sites/default/files/documents/sdg11-synthesis-report-2018-en.pdf> (accessed on 30 January 2024).
2. Europa Nostra. The Venice Manifesto for a European Cultural Citizenship. 2023. Available online: <https://www.europanostra.org/wp-content/uploads/2023/11/2023-Venice-Manifesto-English.pdf> (accessed on 30 January 2024).
3. United Nations. Policy Document for the Integration of a Sustainable Development Perspective into the Processes of the World Heritage Convention. 2015. Available online: <https://whc.unesco.org/document/139747> (accessed on 30 January 2024).
4. United Nations. Transforming our World: The 2030 Agenda for Sustainable Development. 2015. Available online: <https://sdgs.un.org/sites/default/files/publications/21252030%20Agenda%20for%20Sustainable%20Development%20web.pdf> (accessed on 30 January 2024).
5. Hayles, C.; Huddleston, M.; Chinowsky, P.; Helman, J. Climate Adaptation Planning: Developing a Methodology for Evaluating Future Climate Change Impacts on Museum Environments and Their Collections. *Heritage* **2023**, *6*, 7446–7465. [CrossRef]
6. Saba, M.; Golondrino, G.E.C.; Torres-Gil, L.K. A Critical Assessment of the Current State and Governance of the UNESCO Cultural Heritage Site in Cartagena de Indias, Colombia. *Heritage* **2023**, *6*, 5442–5468. [CrossRef]
7. Vardopoulos, I. Adaptive Reuse for Sustainable Development and Land Use: A Multivariate Linear Regression Analysis Estimating Key Determinants of Public Perceptions. *Heritage* **2023**, *6*, 809–828. [CrossRef]
8. Papatzani, S.; Michail, G.; Tzamalís, G.; Skitsas, G. UNESCO Historic Centre (Chorá) of Patmos Island: Conservation and Reconstruction of a Collapsed Urban House. *Heritage* **2022**, *5*, 3100–3132. [CrossRef]
9. Marenčić, Z.B.; Pavlović, R.; Tutek, I. Industrial Heritage of Dubrovnik—Unaffirmed Potential of Gruž Bay. *Heritage* **2022**, *5*, 2332–2369. [CrossRef]
10. Elnaggar, A. Nine principles of green heritage science: Life cycle assessment as a tool enabling green transformation. *Heritage Sci.* **2024**, *12*, 7. [CrossRef]
11. Li, L.; Tang, Y. Towards the Contemporary Conservation of Cultural Heritages: An Overview of Their Conservation History. *Heritage* **2023**, *7*, 175–192. [CrossRef]
12. Xie, K.; Zhang, Y.; Han, W. Architectural Heritage Preservation for Rural Revitalization: Typical Case of Traditional Village Retrofitting in China. *Sustainability* **2024**, *16*, 681. [CrossRef]
13. Rios, A.J. Learning from the Past: Parametrical analysis of cob walls. *Appl. Sci.* **2023**, *13*, 9045. [CrossRef]
14. Jiménez Rios, A.; O’Dwyer, D. Earthen buildings in Ireland. In *6th International Congress on Construction History (6ICCH 2018), Brussels, Belgium, 9–13 July 2018*; Wouters, I., van de Voorde, S., Bertels, I., Espion, B., de Jonge, K., Zastavni, D., Eds.; CRC Press: Boca Raton, FL, USA, 2018; pp. 787–794. Available online: <https://www.taylorfrancis.com/chapters/edit/10.1201/9780429446719-12/earthen-buildings-ireland-jim%C3%A9nez-rios-alejandro-dwyer-dermot> (accessed on 30 February 2024).
15. Sardella, A.; Palazzi, E.; von Hardenberg, J.; Del Grande, C.; De Nuntiis, P.; Sabbioni, C.; Bonazza, A. Risk mapping for the sustainable protection of cultural heritage in extreme changing environments. *Atmosphere* **2020**, *11*, 700. [CrossRef]
16. Briz, E.; Garmendia, L.; Marcos, I.; Gandini, A. Improving the Resilience of Historic Areas Coping with Natural and Climate Change Hazards: Interventions Based on Multi-Criteria Methodology. *Int. J. Arch. Heritage* **2023**, 1–28. [CrossRef]
17. Coisson, E.; Ferrari, L. Emergency Response to Damaged Architectural Heritage: Time, Safety and Conservation. In *Structural Analysis of Historical Constructions*; Endo, Y., Hanazato, T., Eds.; Springer Nature: Cham, Switzerland, 2024; pp. 1320–1331. [CrossRef]
18. Roca, P.; Cervera, M.; Gariup, G.; Pela, L. Structural Analysis of Masonry Historical Constructions. Classical and Advanced Approaches. *Arch. Comput. Methods Eng.* **2010**, *17*, 299–325. [CrossRef]
19. Lagomarsino, S.; Cattari, S. PERPETUATE guidelines for seismic performance-based assessment of cultural heritage masonry structures. *Bull. Earthq. Eng.* **2014**, *13*, 13–47. [CrossRef]
20. Bracchi, S.; Rota, M.; Penna, A.; Magenes, G. Consideration of modelling uncertainties in the seismic assessment of masonry buildings by equivalent-frame approach. *Bull. Earthq. Eng.* **2015**, *13*, 3423–3448. [CrossRef]
21. Tomić, I.; Vanin, F.; Beyer, K. Uncertainties in the Seismic Assessment of Historical Masonry Buildings. *Appl. Sci.* **2021**, *11*, 2280. [CrossRef]
22. D’altri, A.M.; Sarhosis, V.; Milani, G.; Rots, J.; Cattari, S.; Lagomarsino, S.; Sacco, E.; Tralli, A.; Castellazzi, G.; de Miranda, S. Modeling Strategies for the Computational Analysis of Unreinforced Masonry Structures: Review and Classification. *Arch. Comput. Methods Eng.* **2020**, *27*, 1153–1185. [CrossRef]
23. Božulić, I.; Vanin, F.; Beyer, K. Numerical Modeling of FRP-Strengthened Masonry Structures Using Equivalent Frame Models. In *Structural Analysis of Historical Constructions*; Endo, Y., Hanazato, T., Eds.; Springer Nature: Cham, Switzerland, 2024; pp. 400–406. [CrossRef]
24. de Sousa Medeiros, K.A.; Palhares, R.d.A.; Parsekian, G.A.; Shrive, N.G. Simplified frame models to simulate the in-plane load–displacement response of multi-story, perforated, partially grouted masonry walls. *Structures* **2023**, *55*, 2086–2104. [CrossRef]
25. Bertani, G.; Patruno, L.; D’altri, A.; Castellazzi, G.; de Miranda, S. A single-surface multi-failure strength domain for masonry. *Int. J. Solids Struct.* **2024**, *288*, 112624. [CrossRef]

26. Pereira, M.; D’Altri, A.M.; de Miranda, S.; Glisic, B. 3D Non-periodic Masonry Texture Generation of Cultural Heritage Structures. In *Structural Analysis of Historical Constructions*; Endo, Y., Hanazato, T., Eds.; Springer Nature: Cham, Switzerland, 2024; pp. 366–373. [CrossRef]
27. Rios, A.J.; Nela, B.; Pingaro, M.; Reccia, E.; Trovalusci, P. Rotation and sliding collapse mechanisms for in plane masonry pointed arches: Statistical parametric assessment. *Eng. Struct.* **2022**, *262*, 114338. [CrossRef]
28. Rios, A.J.; Pingaro, M.; Reccia, E.; Trovalusci, P. Statistical Assessment of In-Plane Masonry Panels Using Limit Analysis with Sliding Mechanism. *J. Eng. Mech.* **2022**, *148*, 04021158. [CrossRef]
29. Rios, A.J.; Nela, B.; Pingaro, M.; Reccia, E.; Trovalusci, P. Parametric analysis of masonry arches following a limit analysis approach: Influence of joint friction, pier texture, and arch shallowness. *Math. Mech. Solids* **2023**, 10812865231175385. [CrossRef]
30. Prajapati, S.; Shrestha, K.C.; Shakya, M. Seismic fragility evaluation of the Nepalese pagoda temple: A case study of Laxmi Narsingha temple. *J. Build. Eng.* **2024**, *87*, 108993. [CrossRef]
31. Yavartanoo, F.; Kim, T.; Kim, J.; Jang, H.; Kim, C.-S. Out-of-plane behavior of U-shaped unreinforced masonry structures. *J. Build. Eng.* **2024**, *86*, 108984. [CrossRef]
32. Meoni, A.; D’alessandro, A.; Mattiacci, M.; García-Macías, E.; Saviano, F.; Parisi, F.; Lignola, G.P.; Ubertini, F. Structural performance assessment of full-scale masonry wall systems using operational modal analysis: Laboratory testing and numerical simulations. *Eng. Struct.* **2024**, *304*, 117663. [CrossRef]
33. Magenes, G.; Penna, A.; Senaldi, I.E.; Rota, M.; Galasco, A. Shaking Table Test of a Strengthened Full-Scale Stone Masonry Building with Flexible Diaphragms. *Int. J. Arch. Heritage* **2013**, *8*, 349–375. [CrossRef]
34. Guerrini, G.; Senaldi, I.; Graziotti, F.; Magenes, G.; Beyer, K.; Penna, A. Shake-Table Test of a Strengthened Stone Masonry Building Aggregate with Flexible Diaphragms. *Int. J. Arch. Herit.* **2019**, *13*, 1078–1097. [CrossRef]
35. Vintzileou, E.; Mouzakis, C.; Adami, C.-E.; Karapitta, L. Seismic behavior of three-leaf stone masonry buildings before and after interventions: Shaking table tests on a two-storey masonry model. *Bull. Earthq. Eng.* **2015**, *13*, 3107–3133. [CrossRef]
36. Mininno, G.; Ghiassi, B.; Oliveira, D.V. Modelling of the In-Plane and Out-of-Plane Performance of TRM-Strengthened Masonry Walls. *Key Eng. Mater.* **2017**, *747*, 60–68. [CrossRef]
37. Arce, A.; Kapsalis, P.; Papanicolaou, C.G.; Triantafillou, T.C. Diagonal Compression Tests on Unfired and Fired Masonry Wallettes Retrofitted with Textile-Reinforced Alkali-Activated Mortar. *J. Compos. Sci.* **2023**, *8*, 14. [CrossRef]
38. Shabani, A.; Feyzabadi, M.; Kioumars, M. Model updating of a masonry tower based on operational modal analysis: The role of soil-structure interaction. *Case Stud. Constr. Mater.* **2022**, *16*, e00957. [CrossRef]
39. Wang, P.; Milani, G. Specialized 3D Distinct element limit analysis approach for a fast seismic vulnerability evaluation of massive masonry structures: Application on traditional pagodas. *Eng. Struct.* **2023**, *282*, 115792. [CrossRef]
40. Jiao, L.; Taponnier, P.; Mccallum, A.C.-C.; Xu, X. The shape of the Himalayan “Arc”: An ellipse pinned by syntaxial strike-slip fault tips. *Proc. Natl. Acad. Sci. USA* **2024**, *121*, e2313278121. [CrossRef] [PubMed]
41. Bollinger, L.; Adhikari, L.B.; Vergne, J.; Hetényi, G.; Subedi, S. The 2015 April 25 Gorkha Earthquake. In *Himalaya: Dynamics of a Giant, Current Activity of the Himalayan Range*; Wiley: Hoboken, NJ, USA, 2023; Volume 3, pp. 217–237. [CrossRef]
42. Elliott, J.R.; Jolivet, R.; González, P.J.; Avouac, J.-P.; Hollingsworth, J.; Searle, M.P.; Stevens, V.L. Himalayan megathrust geometry and relation to topography revealed by the Gorkha earthquake. *Nat. Geosci.* **2016**, *9*, 174–180. [CrossRef]
43. Xiong, N.; Niu, F.; Wang, R. Significance of Nonplanar Rupture of the Mainshock and Optimal Faulting in Forecasting Aftershocks of the 2015 Mw 7.8 Gorkha Earthquake. *Seism. Res. Lett.* **2020**, *91*, 1606–1616. [CrossRef]
44. Varum, H.; Dumar, R.; Furtado, A.; Barbosa, A.R.; Gautam, D.; Rodrigues, H. Chapter 3—Seismic Performance of Buildings. In *Nepal after the Gorkha Earthquake, in Impacts and Insights of the Gorkha Earthquake*; Gautam, D., Rodrigues, H., Eds.; Elsevier: Amsterdam, The Netherlands, 2018; pp. 47–63. [CrossRef]
45. UNESCO. 45 COM Convention Concerning the Protection of the World Cultural and Natural Heritage. 2023. Available online: <https://whc.unesco.org/archive/2023/whc23-45com-7B-en.pdf> (accessed on 20 February 2024).
46. Saisi, A.; Borlenghi, P.; Gentile, C. Between Safety and Conservation—Procedure for the Assessment of Heritage Buildings Based on Historic Research. *Buildings* **2023**, *13*, 2236. [CrossRef]
47. Roca, P. The Icarsah Guidelines on the Analysis, Conservation and Structural Restoration of Architectural Heritage. In Proceedings of the 12th International Conference on Structural Analysis of Historical Constructions (SAHC), Barcelona, Spain, 29 September–1 October 2021. Available online: https://www.scipedia.com/public/Roca_2021a (accessed on 20 February 2024).
48. Ranjitkar, R.K.; Joshi, L. Lakshmi Narayan Temple Kathmandu Darbar Initiative Final Report. 2004. Available online: https://danam.cats.uni-heidelberg.de/files/danam-cms/Lakshmi_Narayan_Temple_KDI_Final_Report_DyGUJ9h.pdf (accessed on 30 January 2024).
49. Mishra, M.; Lourenço, P.B. Artificial intelligence-assisted visual inspection for cultural heritage: State-of-the-art review. *J. Cult. Herit.* **2024**, *66*, 536–550. [CrossRef]
50. Bayraktar, A.; Hökelekli, E. Seismic Performances of Different Spandrel Wall Strengthening Techniques in Masonry Arch Bridges. *Int. J. Arch. Heritage* **2020**, *15*, 1722–1740. [CrossRef]
51. Parajuli, H.R. Determination of mechanical properties of the Kathmandu Valleey world heritage brick masonry buildings. In Proceedings of the 15 World Conference on Earthquake Engineering, Lisbon, Portugal, 24–28 September 2012. Available online: https://www.iitk.ac.in/nicee/wcee/article/WCEE2012_3139.pdf (accessed on 30 January 2024).

52. Parajuli, H.R.; Maskey, P.N.; Kiyono, J. Disaster Risk Management for the Historic City of Patan, Nepal, Final Report of the Kathmandu Research Project. 2012. Available online: https://r-dmuch.jp/wp/assets/en/project/dl_files/report/2012+03+KTM+Final+Report.pdf (accessed on 20 February 2018).
53. Gavrilovich, P.; Pichard, P. Methodology for strengthening and repair of earthquake damaged monuments in Pagan—Burma. In Proceedings of the Eight World Conference on Earthquake Engineering, San Francisco, CA, USA, 21–28 July 1984. Available online: https://www.iitk.ac.in/nicee/wcee/article/8_vol1_609.pdf (accessed on 20 February 2018).
54. Jaishi, B.; Ren, W.X.; Zong, Z.H.; Maskey, P.N. Dynamic and seismic performance of old multi-tiered temples in Nepal. *Eng. Struct.* **2003**, *25*, 1827–1839. [[CrossRef](#)]
55. William, K.; Warnke, E. Constitutive model for the triaxial behaviour of concrete, in IABSE reports of the working commissions = Rapports des commissions de travail AIPC = IVBH Berichte der Arbeitskommissionen. In Proceedings of the Seminar on Concrete Structures Subjected to Triaxial Stresses, Bergamo, Italy, 17–19 May 1974; pp. 1–30. [[CrossRef](#)]
56. ANSYS Inc. *ANSYS Mechanical APDL Feature Archive*; ANSYS Inc.: Canonsburg, PA, USA, 2023.
57. Rios, A.J.; O’Dwyer, D. Numerical modelling of cob’s non-linear monotonic structural behaviour. *Int. J. Comput. Methods* **2020**, *17*, 1940013. [[CrossRef](#)]
58. Altunişik, A.C.; Genç, A.F.; Günaydin, M.; Okur, F.Y.; Karahasan, O. Dynamic response of a historical armory building using the finite element model validated by the ambient vibration test. *J. Vib. Control.* **2018**, *24*, 5472–5484. [[CrossRef](#)]
59. Sinaei, S.; Abadi, E.I.Z.; Hoseini, S.J. Failure Analysis of Skewed Persian Brick Masonry Barrel Vaults: Experimental and Numerical Study. *J. Perform. Constr. Facil.* **2023**, *37*, 04023057. [[CrossRef](#)]
60. Hejazi, M.; Soltani, Y. Parametric study of the effect of hollow spandrel (Konu) on structural behaviour of Persian brick masonry barrel vaults. *Eng. Fail. Anal.* **2020**, *118*, 104838. [[CrossRef](#)]
61. Shabani, A.; Kioumars, M. Seismic assessment and strengthening of a historical masonry bridge considering soil-structure interaction. *Eng. Struct.* **2023**, *293*, 116589. [[CrossRef](#)]
62. Shakya, M. Modal Analysis Using Ambient Vibration Measurement and Damage Identification of Three Tiered Radha Krishna Temple. 2010. Available online: https://www.researchgate.net/publication/260096970_MODAL_ANALYSIS_USING_AMBIENT_VIBRATION_MEASUREMENT_AND_DAMAGE_IDENTIFICATION_OF_THREE_TIERED_RADHA_KRISHNA_TEMPLE (accessed on 20 February 2018).
63. Takai, N.; Shigefuji, M.; Rajaure, S.; Bijukchhen, S.; Ichyanagi, M.; Dhital, M.R.; Sasatani, T. Strong ground motion in the Kathmandu Valley during the 2015 Gorkha, Nepal, earthquake. *Earth Planets Space* **2016**, *68*, 10. [[CrossRef](#)]
64. *IS:1905-1987*; Code of Practice for Structural Use of Unreinforced Masonry. Bureau of Indian Standards: New Delhi, India, 1987. Available online: <https://archive.org/details/gov.in.is.1905.1987> (accessed on 20 February 2018).
65. European Commission. Industry 5.0: Human-Centric, Sustainable and Resilient. 2020. Available online: <https://op.europa.eu/en/publication-detail/-/publication/aed3280d-70fe-11eb-9ac9-01aa75ed71a1> (accessed on 30 January 2024).

Disclaimer/Publisher’s Note: The statements, opinions and data contained in all publications are solely those of the individual author(s) and contributor(s) and not of MDPI and/or the editor(s). MDPI and/or the editor(s) disclaim responsibility for any injury to people or property resulting from any ideas, methods, instructions or products referred to in the content.